International Journal of Mass Spectrometry 313 (2012) 36–40

Contents lists available at SciVerse ScienceDirect

International Journal of Mass Spectrometry

journal homepage: www.elsevier.com/locate/ijms

Rotation of focal plane of magnetic analyzer in an isotope ratio mass spectrometer using curved shims

Rajender K. Bhatia*, Yogesh Kumar, K. Prathap Reddy, V.K. Yadav, E. Ravisankar, T.K. Saha, V. Nataraju, V.K. Handu

Technical Physics Division, BARC, Mumbai 400085, India

ARTICLE INFO

Article history:
Received 18 February 2011
Received in revised form
12 December 2011
Accepted 21 December 2011
Available online 29 December 2011

Keywords:
Curved shims
TIMS
Focal plane
Magnetic analyzer
Faraday collector

ABSTRACT

The inclination of focal plane from beam axis of the magnetic sector analyzer in an isotopic ratio mass spectrometer is an important design feature. For a stigmatic geometry mass spectrometer, the focal plane is normally inclined by an angle of ~25° with respect to the principal trajectory which presents various complications in case the number of collectors is more than five. An attempt has been made by us to rotate this plane along a line normal to the principal trajectory (by using shims on exit side of magnetic analyzer) resulting in ease of design for the collector system. This paper presents theoretical explanation, computer simulation and experimental results on this development. Simulated results on optimum shim curvature are in good agreement with experimental data.

1. Introduction

A thermal ionization mass spectrometer [1] (TIMS-2) is being developed for geo-chronological applications based on an earlier design of system (TIMS-1) with specifications given in Table 1 of supplementary information (SI). A multi-collector system with seven faraday cups is desirable for carrying out isotopic ratio measurements on elements ranging from Sr to Pu while the earlier system (TIMS-1) had only three collectors. Ion optical parameters of the mass spectrometer decide the exact locations and separations of these collectors and multi-isotope analysis demands the adjustment of these detectors across the focal plane that normally makes an inclination of 25° to the principal beam axis. This necessarily makes the collector system very bulky and unwieldy, particularly, if large number of collectors is required. One of the ways to simplify the collector positioning and movement mechanism is to redesign the magnet so as to rotate the focal plane of the image along a line normal to the principal beam axis. Various other methods have also been used to rotate the focal plane. For example, in Ref. [2] two quadrupoles: an electrostatic quadrupole at the detector side and a magnetic one at the source side of the sector magnet have been used. In Ref. [3], magnet (exit) pole face with curvature has been suggested for this purpose and it has been shown that exit curvature may be used to make focal plane normal to principal beam axis. Further, existing theory [4,5] has been used for calculation of optimum exit curvature. However, the theory does not fully account for fringe fields and an experimental optimization of exit curvature is desirable. For experimental optimization, attachment of a shim at exit boundary is more convenient (compared to fabrication of magnet with curvature of pole faces) as many shims of different curvature may be easily fabricated and evaluated. In this study, we have used theory [4,5] to determine optimum exit curvature that has been further optimized experimentally by attaching shims of different curvature. Since, theory does not adequately take fringe fields into account, optimum curvature has also been determined by computer simulation. Computer simulations also have advantage of being able to consider different field in the shim region which may occur due to small insulation gap between shim and the magnet boundary. Theoretical calculations showed optimum exit shim curvature of 177 mm while computer simulations taking fringe field into account, showed an optimum curvature of 160 mm. Variation of magnetic field in the shim region was experimentally measured and field was found to be lower by 200 Gauss. Simulations using this field variation showed optimum shim curvature of 140 mm. Experiments carried out with shims of different curvature showed good agreement with simulation data with an optimum curvature of 130 mm.

A concave curvature at exit boundary has the drawback of increasing the spherical aberration. This may be reduced by using a shim at entrance boundary with convex curvature. Optimum

* Corresponding author. Tel.: +91 2225592409; fax: +91 22025505296.
E-mail address: raj@barc.gov.in (R.K. Bhatia).

1387-3806/$ – see front matter © 2011 Elsevier B.V. All rights reserved.
doi:10.1016/j.ijms.2011.12.013

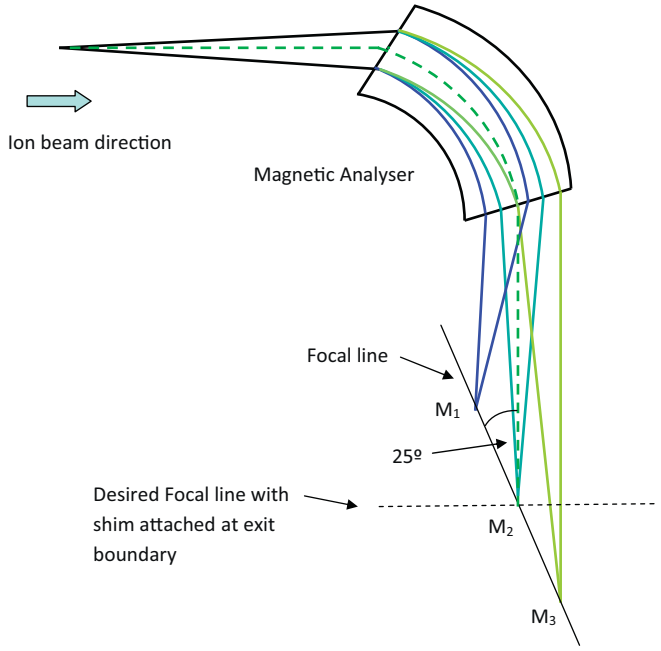

Fig. 1. Schematic diagram showing the inclined focal line for typical magnetic analyzer using ions of three different masses ($M3 > M2 > M1$). A desirable focal line for convenient placement of collectors is also shown.

curvature at entrance boundary has been determined theoretically and experimental results with shims at both entrance and exit boundaries have been presented.

2. Theory

The image distances (from magnet edge) for ion beams of different masses, depend on ion optical parameters of the analyzer viz., radius of ion beam trajectory, angle of deflection and entry and exit angles [5,6]. Typically, in a magnetic sector mass spectrometer, ions of different masses focus at different distances from magnet resulting in focal plane not being normal to beam axis as shown in Fig. 1. In the following, we theoretically determine if a concave curvature (as seen from outside) of magnet at exit boundary helps in rotating the focal plane normal to beam axis (shown as 'desired plane' in Fig. 1).

First we consider focusing of ions of a particular mass in magnetic analyzer with straight boundaries as schematically shown in supplementary information (SI). Trajectory of ions with different velocities and angles (α) to central beam is given by [5]:

$$Y = r\{M_1\alpha + M_2\,\beta + M_{11}\alpha^2 + M_{12}\,\alpha\,\beta + M_{22}\,\beta^2\} + X\{N_1\alpha + N_2\beta + N_{11}\alpha^2 + N_{12}\alpha\beta + N_{22}\beta^2\} \quad (1)$$

where r is radius of curvature of principal trajectory of ions, Y is the displacement with respect to principal axis after deflection, β is the relative variation in velocity of the ion beam with respect to mean velocity ($\beta = \Delta v/v_0$ where v_0 is average velocity of ions and Δv is variation from v_0), X is the position along principal axis with respect to the exit edge of the magnet. Different coefficients M and N depend on the shape and dimensions of the magnetic sector analyzer. These parameters have been derived for homogeneous magnetic field for any curvature of boundaries [5,7,8] and the values as given by Hintenberger and König [5] have been used here.

Considering only the first order terms of α (first order focusing) and $\beta = 0$ in Eq. (1), image distance (S_i) from the exit boundary of the magnet (using values of parameters given in Ref. [5]) is given by:

$$S_i = \frac{[S_o(\cos\Phi + t_1\,\sin\Phi) + (r\,\sin\Phi)]}{[(S_o/r)[\sin\Phi - (t_1+t_2)\cos\Phi - (t_1t_2\,\sin\Phi)] - \cos\Phi - (t_2\,\sin\Phi)]} \quad (2)$$

where S_0 is the object distance, Φ is the bending angle of the magnet, $t_1 = \tan\epsilon_1$ and $t_2 = \tan\epsilon_2$, ϵ_1 and ϵ_2 are entry and exit angles of the principal ion beam trajectory with respect to normal at entry and exit boundary of the magnet, respectively.

For finding focal plane orientation we need to determine focusing distance of ions with different masses. If r_0, ϵ_{20} and Φ_0 are the radius of curvature, exit angle and deflection angle for central mass (M_0), we may write radius of curvature (r), exit angle (ϵ_2) and deflection angle (Φ) for arbitrary mass (M) by [9]:

$$\Phi = \Phi_0 + d\Phi = \Phi_0 + (M_0/M)^{1/2}[1 - (M/M_0)^{1/2} + (1 - (M/M_o)^{1/2}\,\cos((M_0/M)^{1/2} - 1))t_2]$$
$$r = r_0(M/M_0)^{1/2}$$
$$\epsilon_2 = \epsilon_{20} - d\Phi$$

The spherical aberration (Y_s) for first order focusing as derived from Eq. (1) is given by [5]:

$$Y_s = \left(M_{11} - \left(\frac{M_1}{N_1}\right)\,N_{11}\right) r\alpha^2 \quad (3)$$

In some of the earlier studies, possibility of rotation of image plane by variation of geometric parameters of the magnetic analyzer has been discussed [10–14]. In present study we have added a shim at exit of magnet to rotate the focal plane and another shim at entrance of the magnet to minimize aberrations. Effect of shim on focal plane and aberration has been determined in the following.

2.1. Effect of exit boundary curvature on image plane

The curvature on the exit boundary provides an extra magnetic region on both sides of the central mass and hence the exit and bending angles for masses other than the central beam are altered as schematically shown in Fig. 2 (for $M > M_0$). It is seen that exit angle (angle of ion trajectory with respect to normal to boundary at exit point) reduces for $M > M_0$ which in turn results in shifting of the focal point towards the magnet. On the other hand for $M < M_0$, the focal points shifts away from the magnet. This results in rotating the focal line counter clockwise as desired to make it normal to ion trajectory (see Fig. 1). The addition of shim also increases the deflection angle slightly (angle Φ' in Fig. 2). But the effect of slight alteration of deflection angle is negligible as compared to that of exit angle.

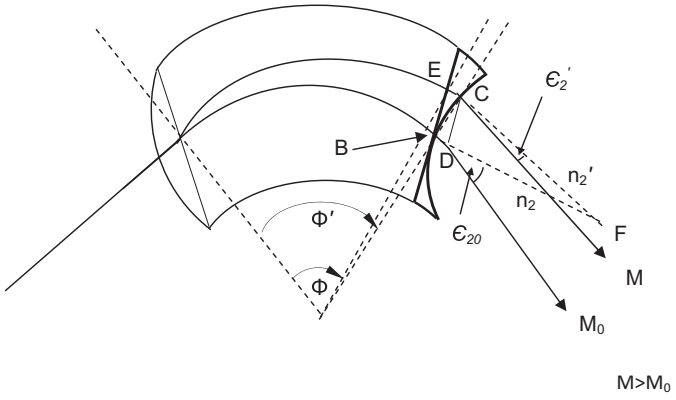

Fig. 2. Schematic diagrams showing central ion beam trajectories for ions of different masses with exit shims attached.

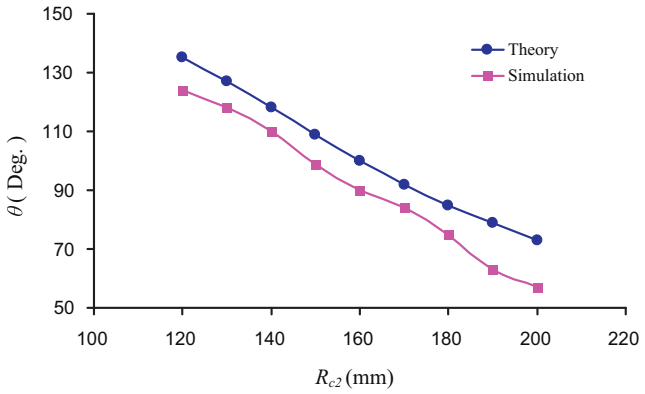

Fig. 3. Theoretical and simulation results on the variation of focal line angle (θ) with radius of curvature (R_{c2}) of exit side shim.

On attachment of a shim with curvature R_{c2} (=*FB* in Fig. 2) and approximation $dr \ll R_{c2}$, the modified exit angle (ϵ_2') and deflection angle (Φ') for different masses are given by:

$$\Phi' = \Phi + \frac{EC}{r} = \Phi + \frac{[R_{c2} - (R_{c2}^2 - dr^2)^{1/2}]}{r} \quad (4)$$

$$\epsilon_2' = \epsilon_2 - \sin^{-1}\left(\frac{dr}{R_{c2}}\right) + d\Phi \quad (5)$$

These modified parameters have been used in Eq. (2) and the resulting image distances have been calculated for different ion masses and shims of different radii. For given shim curvature, focal line inclination was determined using image distances for different ion masses. The results obtained (for $\epsilon_1 = 26.56^\circ$ and $S_0 = 600$ mm used in our system) are shown in Fig. 3. Here θ denotes angle between focal line and principal beam axis. It is seen that the inclination of focal line is 90° to the principal beam axis for exit shim curvature of 177 mm.

2.2. Effect of shim on entry boundary of magnet

The exit boundary with concave curvature (as seen from outside) with suitable radius rotates the focal plane at desired angle as explained above. However, it has the drawback of increasing the spherical aberration thereby reducing the resolving power of the magnet. The aberration due to any curvature on entry and exit side can be calculated using Eq. (3). As per the equation the spherical aberrations can generally be reduced by using suitable magnet curvatures on entry and exit boundaries of the magnet. Since in our case concave type of curvature is used on exit side, the additional aberration due to this can be circumvented by using a shim with convex curvature of suitable radius on the entry side. Using modified parameters from Eqs. (4) and (5) in (3), the beam width at the focal point has been calculated. Fig. 4 shows the dependence of beam width (W_B) at focal point on entry shim curvature (R_{c1}) for

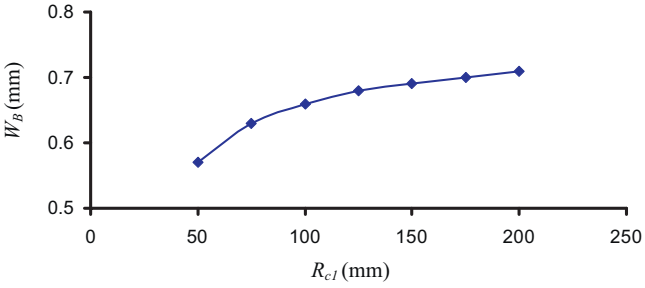

Fig. 4. Effect of entrance shim curvature (R_{c1}) on beam width (W_B) at focal point.

Table 1
Calculation of image distance for $R_{c1} = 100$ mm, $R_{c2} = 177$ mm and $\epsilon_1 = 26.56^\circ$.

M (amu)	ϵ_2' (°)	Φ' (°)	S_i (mm)
210	37.1	95.0	592.6
220	32.7	92.9	597.2
230	28.5	90.9	599.5
235	26.6	90.0	599.9
240	24.6	89.1	599.8
250	21.0	87.4	598.2
260	17.4	85.8	594.8
270	14.1	84.3	590.2

fixed exit shim curvature of 177 mm. It is seen that small value of R_{c1} is desirable for suppressing the aberration and hence improving the resolution. However, we have restricted R_{c1} to 100 mm as further lowering of the radius of curvature at entry will make the location of the magnet very critical. This is because the entry angle depends on beam entry location for a curved boundary. Calculations showed that entry shim radius has no effect on the orientation of focal plane and only helps in reducing aberration. The results of calculations using 100 mm convex shim at entry and 177 mm concave shim at exit are shown in Table 1. It is observed that distance of focusing from magnet edge (S_i) for masses 210–270 amu has variation of ±5 mm (and a mean distance of 595 mm) which is negligible and hence the focal line can be considered as normal to beam axis.

3. Computer simulation

Computer simulation studies using software package SIMION 7.0 [15] have been carried out to determine effect of exit shim curvature on focal plane. The exit curvature of the magnet was varied in the range of 100–200 mm with a step size of 10 mm and movement of ion groups was analyzed with a central mass of 235 amu and mass-band of ±35 amu. The slope of the line joining focal points for all the masses was determined using the position co-ordinates of the extreme ends of this line. The calculated slope has been plotted against the radius of curvature in Fig. 3. From the graph it is clear that the focal line is almost normal to principal axis for a curvature radius of 160 mm. Difference in optimum radius of curvature of 160 mm by computer simulation and 177 mm by theoretical calculations is mainly attributed to better accounting of fringe field by simulation package.

4. Experimental

Experiments were carried out by attaching metallic shims made of mild steel (photograph shown in supplementary information) with different radii in the range from 100 mm to 200 mm in steps of 10 mm at the exit boundary of the magnet. These shims were fabricated in house with one side as flat and other with required curvature. The flat side of the shim was attached to magnet boundaries (which are also flat) using non magnetic adhesive in such a way that there is minimum air gap. The pole gap uniformity between the lower and upper parts (north and south poles) of shims was ensured by using 304 stainless steel (non magnetic) spacers (tolerance better than 10 μm) with height equal to that of pole gap of magnet.

Peak shapes of Re-187 ion beam were recorded for each curvature on a single movable collector at various locations across the line normal to the ion beam axis (by changing the magnetic field). Base widths of these peaks were measured at 10% of the maximum peak height in terms of magnet current (72 mA in Fig. 5). Lower base width indicates smaller beam width at the focal point. The base width is expected to be independent of location if the beam focuses on this line. Taking the mean position on the beam axis as zero, the peak shapes were recorded from −13 mm (low mass side)

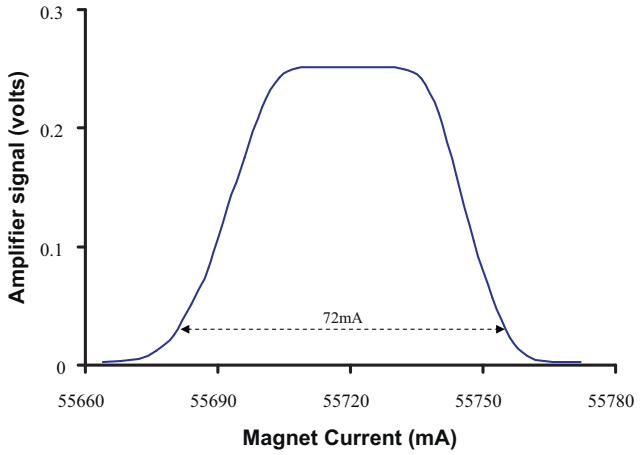

Fig. 5. Peak shape for rhenium ion beam on single collector located at centre of the line normal to principal beam axis; R_{c1} = 100 mm, R_{c2} = 130 mm.

to +13 mm (high mass side). To suppress the additional aberration, a convex curvature of 100 mm radius was attached to the entry boundary of the magnet. Effect of shim at entry boundary was also studied by recording peak shapes with and without entry shim for optimum exit shim.

5. Results and discussion

Peak shapes determined on different positions of line normal to principal beam axis (with entrance shim radius of 100 mm) showed minimum variation for exit shim radius of 130 mm. Shape of peak obtained at center position for optimum exit shim is shown in Fig. 5 for rhenium ions. In this case, the variation of base width at different points (±13 mm) on normal line was found to be 72–78 mA. We may add that the beam width at collector location was 0.70 mm without any shim, it increased to ~0.86 mm on use of exit shim of 130 mm diameter and then reduced to 0.74 mm on use of both entry and exit shims.

Having found optimum entry and exit shims, seven collectors with positions suitable for analysis of Nd were installed on a line normal to principal beam axis. Results obtained for simultaneous collection of Nd isotopes are shown in Fig. 6. Uniformity of peak shapes on all collectors confirms the rotation of focal plane along the line normal to the central ion beam.

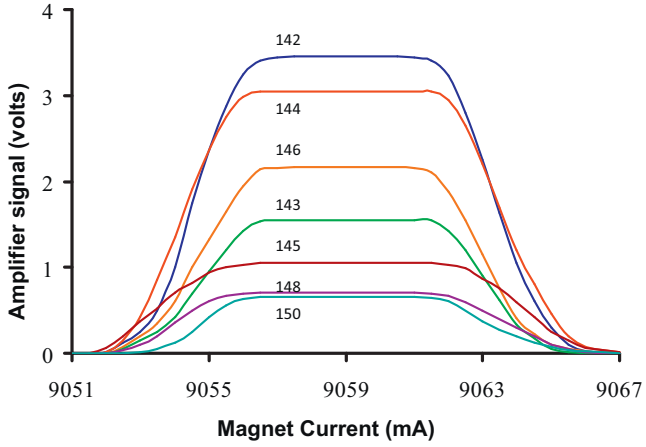

Fig. 6. Peak shapes for seven isotopes of Nd collected simultaneously on seven collectors placed on a line normal to principal beam axis with R_{c1} = 100 mm and R_{c2} = 130 mm; all the different peak heights are as per the abundance of different Nd isotopes.

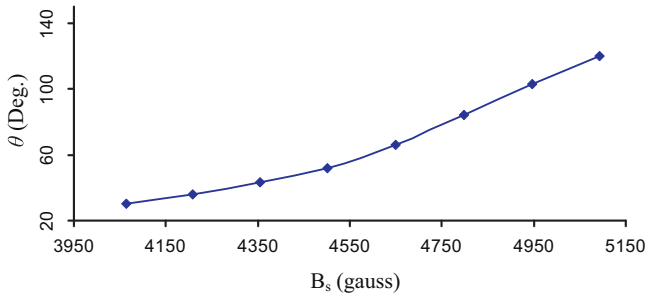

Fig. 7. Effect of magnetic field in shim region (B_s) on focal line angle (θ).

The differences of optimum shim radius of curvature between theoretical calculations, simulations and experimental results may be due to the fringe field distribution of the magnetic field and slightly different magnetic field in the shim region that may arise due to small gap between magnet and shim as well as shim material being different from main magnet material. The theoretical calculations are based on sharp cutoff approximation, i.e., field is constant up to a virtual field boundary located at a distance of approximately 1–2 pole gaps from pole edges. However, in real conditions the field is extended to considerable distances from the pole boundaries. The effect of extended fringe field has been studied by Enge and co-workers [16,17] whereby it is stated that it alters the entry and exit angles and hence the focusing condition of the ion beams. The fringe field is better accounted for in computer simulations resulting in better agreement with experimental data. The agreement of simulation to experimental data is further improved when difference in magnetic field in shim region compared to that in main magnet is taken into account. For this purpose, the actual magnetic field profile was measured using hall probe. From the profile it was found that the field in the shim region is less by around 200 gauss compared to that expected for ideal field profile (for a central magnetic field of 5000 gauss). To see the dependence of different magnetic fields in shim region on the focal plane rotation angle, simulations have been carried out for a field of 5000 gauss in the main magnet region and different fields in the shim region. The results are shown in Fig. 7. It shows that there is a variation of around 20° in the focal plane angle for a field difference of 200 gauss in the shim region. The variation of 20° corresponds to 20 mm in R_{c2} as per Fig. 3 which means that the optimum radius will be 140 mm (instead earlier simulation value of 160 mm) in a good agreement with experimental value of 130 mm. A small difference of 10 mm could be due to different fringe field distribution in simulation and in practical case (which is difficult to verify experimentally) and also due to small unavoidable gap between main magnet and the shim.

It is recommended in US patent [3] that curvatures on the pole boundaries should ideally be introduced by removing the material for convex curvature on entry so that the deflection angle of the magnet is not altered. However, in the present study, a shim has been added to existing magnet as it facilitates the experimental optimization of shim curvature as discussed in the introduction. The quality of the peak shapes shown in Fig. 6 indicates that there is no adverse effect due to this procedure.

Further to check any effect on performance of the instrument, isotopic ratio measurement for strontium standard sample (SRM 0978) was carried out for 87/86 ratio. The sample was deposited on the side rhenium filaments of triple filament assembly. The data was collected in 10 blocks of 10 ratios each for same assembly which provides the internal precision of the measurements. The same sample was analyzed on ten separate filament assemblies on turret for external precision calculation. Table 2 of supplementary information shows the average ratio (87/86) measured on each

assembly. These results are quite closer to those obtained with the conventional instruments with straight boundary magnetic analyzer.

6. Conclusions

The experimental study on rotation of focal plane has provided the optimized radii of curvature for the shims on entry and exit edge of the magnet for rotation of the focal plane along the normal to principal beam axis. The difference between the theoretical, simulated and the experimental values may be attributed to the difference in fringe field distribution and gap between shim and main magnet. This will facilitate compactness of collector chamber and easy location of the collectors in case of large number of collectors. Experiments on Sr 87/86 ratio show that the errors introduced in the system (on addition of shims to rotate focal line) are negligible and do not adversely affect the performance of the instrument.

Acknowledgements

Authors wish to thank Dr. S. Kailas Director, Physics Group, BARC for their constant support for this work. They also gratefully acknowledge Dr. S.K. Gupta Head, Technical Physics Division, BARC for his support in preparing the manuscript in the final form. The contribution from all the team members is thankfully acknowledged.

Appendix A. Supplementary data

Supplementary data associated with this article can be found, in the online version, at doi:10.1016/j.ijms.2011.12.013.

References

[1] Design enhancements of TIMS for geochronological applications at AMD, Hyderabad, in: Proceedings of 11th ISMAS Symposium 'TRICON' 2009, Hyderabad, India, 2009.
[2] H.H. Tuithof, A.J.H. Boerboom, Int. J. Mass Spectrom. Ion Phys. 20 (1976) 107–121.
[3] J.S. Cottrell, P.J. Turner, J. David, United State Patent no. 4,524,275.
[4] H.A. Enge, Deflecting magnets, in: A. Septier (Ed.), The Focusing of Charged Particles, Academic Press, New York, 1967, pp. 203–263.
[5] H. Hintenberger, L.A. König, Advances in Mass Spectrometry, Pergamon Press, New York, 1959, pp. 16–35.
[6] L.A. Konig, H. Hinterberger, Nucl. Instrum. 3 (1958) 133.
[7] H. Hintenberger, L.A. Konig, Z. Naturforsch 11a (1956) 1039.
[8] L.A. Konig, H. Hintenberger, Z. Naturforsch 12a (1957) 377.
[9] V.V.K. Rama Rao, Int. J. Mass Spectrom. 145 (1/2) (1995) 45.
[10] I. Chavet, Nucl. Instrum. Methods 99 (1972) 115–119.
[11] S.I. Warshaw, Nucl. Instrum. Methods 72 (1969) 5.
[12] P. Bounin, Rev. Sci. Instrum. 38 (1967) 1305.
[13] H. Liebl, Optik 16 (1959) 19.
[14] H. Wollnik, Nucl. Instrum. Methods 53 (1967) 197.
[15] D.A. Dahl, SIMION Version 7.0, Idaho National Engineering Laboratory, 2000.
[16] H.A. Enge, Rev. Sci. Instrum. 35 (1964) 278–288.
[17] H. Wollnik, H. Ewald, Nucl. Instrum. Methods 36 (1965) 93.